Neoplasma 2024; 71(6): 544–558

doi:10.4149/neo_2024_240719N305

MTHFD2 promotes breast cancer cell proliferation through IFRD1 RNA m6A methylation-mediated HDAC3/p53/mTOR pathway

Qingqing ZHANG[1,#], Jun MAO[2,#], Luhan XIE[1,#], Ying LU[2], Xiaobo LI[1], Xiaotang YU[1,*], Lianhong LI[1,*]

[1]Department of Pathology and Forensic Medicine, College of Basic Medical Sciences, Dalian Medical University, Dalian, China; [2]Institute of Cancer Stem Cell, Dalian Medical University, Dalian, China

**Correspondence: zqqjdy2014@sina.com; leahyxt@163.com*
[#]Contributed equally to this work.

Received July 19, 2024 / Accepted December 17, 2024

MTHFD2 is highly overexpressed in breast cancer tissues, indicating that it might be used as a target in breast cancer treatment. This study aims to determine the role of MTHFD2 in breast cancer cell proliferation and the molecular pathways involved. In order to investigate MTHFD2 gene expression and its downstream pathways in breast cancer, we started our inquiry with a bioinformatics analysis. We then engineered breast cancer cell lines with either silenced or overexpressed MTHFD2 to study its effects on the cell cycle, proliferation, and the m6A methylation status of the gene IFRD1, predicted as a downstream target. Overexpression of MTHFD2 enhanced cellular proliferation, increased the proportion of EdU-positive cells, and accelerated progression into the S+G2/M phase. In contrast, MTHFD2 knockdown led to opposite effects. MTHFD2 and IFRD1 expression levels showed a strong positive association. Increased MTHFD2 activity boosted HDAC3 and mTOR phosphorylation, activating p70 S6K and 4EBP1-key regulators of cell proliferation. Moreover, overexpression of MTHFD2 was associated with reduced p53 acetylation and total protein levels. Silencing MTHFD2 decreased m6A methylation of IFRD1 RNA, whereas its overexpression increased methylation. Notably, IFRD1 siRNA transfection reversed the proliferative effects induced by MTHFD2 overexpression. Furthermore, MTHFD2 knockdown enhanced the sensitivity of breast cancer cells to several chemotherapeutic agents. In conclusion, MTHFD2 influences breast cancer cell proliferation by modulating the m6A methylation of IFRD1 RNA, which regulates the HDAC3/p53/mTOR pathway. These findings suggest that MTHFD2 inhibitors may synergistically enhance the efficacy of existing chemotherapies.

Key words: GSEA analysis; RNA methylation; m6A methylation RIP assay; combination chemotherapy

Breast cancer, the most prevalent cancer globally, affects millions annually. Despite systemic therapies improving the five-year survival rate to 90%, patients with advanced metastasis face a poor prognosis, with recurrence and metastasis being the leading causes of mortality [1]. Improving clinical diagnosis and treatment approaches requires a thorough understanding of the genetic and molecular pathways underlying breast cancer.

Methylenetetrahydrofolate dehydrogenase (NADP+ Dependent) 2, or MTHFD2, a key enzyme in mitochondrial folate metabolism, is predominantly expressed in rapidly dividing cells, including cancer tissues [2]. This enzyme supports nucleotide synthesis and redox balance, which is essential for the proliferation potential of cancer cells [3]. Research has shown that MTHFD2 is significantly overexpressed in breast cancer compared to normal tissues, which correlates with poor survival outcomes [4]. MTHFD2's overexpression not only facilitates folate metabolism but also impacts cancer cell behavior by promoting proliferation through the AKT signaling pathway, particularly in breast cancer cell lines like MCF-7 [5], and inhibiting the proliferation, migration, and invasive capabilities when targeted [6]. Silencing MTHFD2 can significantly increase the expression of lipid peroxide ROS and inhibit GPX4 protein in breast cancer cells, thereby inducing iron death in breast cancer cells [7]. Zhang et al. [8] suggested in their study that overexpression of MTHFD2 could increase the production of nicotinamide adenine dinucleotide phosphate in breast cancer cells and inhibit the accumulation of intracellular ROS, thus promoting the growth of breast cancer cells. Although MTHFD2 is considered to be an important enzyme protein, which is mainly localized in mitochondria, this is also the main functional direction of the above studies aimed at MTHFD2 mediating breast cancer progression.

In addition to the localization of mitochondria, MTHFD2 is also present in the site of DNA synthesis in the nucleus, and overexpression of MTHFD2 promotes cell proliferation in a way independent of the enzyme's dehydrogenase activity [9]. For example, it may be necessary for cycle regulation. However, how it functions inside the cell nucleus is unknown. In this study, bioinformatics techniques (derived from the GEO database and GSEA analysis techniques) were used to analyze the regulatory relationship of MTHFD2 to Interferon Related Developmental Regulator 1 (IFRD1), a downstream key target unrelated to enzyme dehydrogenase activity. GSEA analysis of MTHFD2-related genes in breast cancer patients suggests that the mTOR pathway and IFRD1 are key pathways and regulatory genes. mTOR plays a significant role in the regulation of cell growth and cycle in breast cancer. Inhibition of the mTOR pathway is also beneficial in restoring breast cancer sensitivity to tamoxifen [10].

Therefore, this study aims to explore whether MTHFD2 affects the mTOR pathway through IFRD1, thereby affecting the abnormal proliferation of breast cancer cells and their sensitivity to chemotherapy drugs. Furthermore, the specific regulatory relationship between MTHFD2 and IFRD1 was further verified with cell transfection siRNA and other technologies, and the critical bridging role of IFRD1 between MTHFD2 and mTOR was analyzed.

Patients and methods

Analysis of correlation between MTFHD2 and breast cancer. MTHFD2 expression levels in breast cancer may be analyzed using the ENCORI website (https://rnasysu.com/encori/panCancer.php) [11]. Search for "MTHFD2" to retrieve its expression data, specifically in breast cancer tissues. On the ProteinAtlas website (https://www.proteinatlas.org/) [12], an analysis of the MTHFD2 expression level relationship with the prognosis of breast cancer was performed.

Fifty-one paired fresh tissues of breast cancer and adjacent normal breast tissues admitted to our hospital between January 2021 and May 2022 were collected. Nineteen stage I cases, 20 stage II cases, and 12 stage III cases were involved. The samples were collected from the Second Affiliated Hospital of Dalian Medical University. All of the samples had been histologically confirmed. None of the patients from whom the specimens were obtained had received chemotherapy and radiotherapy before surgery. The expression level of MTHFD2 protein in tissue samples was detected by immunohistochemistry and was associated with clinicopathological factors (age, tumor size, tumor grade, lymph node metastasis, recurrence level, etc.). The immunohistochemical method was carried out according to the study of Gao et al. [13]. This study and experiment were approved by the Ethics Committee of Dalian Medical University [approval number:2021006].

Cell culture. Human mammary epithelial cells (HMEC and Du4475) and human breast cancer cells (MCF-7, MDA-MB-231, MDA-MB-468, and ZR-75-1) were obtained from Zhejiang Ruoyao Biotech Co., Ltd., (Ningbo, China). The cells were incubated at 37 °C in a humidified environment with 5% CO_2, appropriate for cell passaging, using DMEM supplemented with 10% fetal bovine serum.

qRT-PCR. The Trizol technique was utilized to extract RNA, and 2 mg of mRNA were reverse-transcribed into cDNA. Zhou et al.'s guidelines were followed in the qPCR approach, which used the 7500 Fast Real-Time PCR System (Applied Biosystems; Thermo Fisher Scientific, Inc.) [14].

The $2^{(-\Delta\Delta CT)}$ method [15] was used to calculate the relative expression of target genes. The specific formula of the 2–ΔΔCt method is as follows: ΔCT = CT (target gene) – CT (internal reference gene); ΔΔCT = ΔCT (experimental group) – ΔCT (control group); relative expression = $2^{(-\Delta\Delta CT)}$.

Where CT represents the Cycle Threshold, the number of cycles experienced when the fluorescence signal reaches the set threshold in the PCR reaction. The target gene is the gene you are interested in, and the reference gene is the control gene used to standardize the expression of the target gene.

Primer sequences used were MTHFD2 Forward: 5'-TGAGTGTGATCCTGGTTGGC-3', MTHFD2 Reverse: 5'-TGTCTCACTGTTGATTCCCACAT-3'; IFRD1 Forward: 5'-TCGTTTTCGATCACA GCTCTTC-3', IFRD1 Reverse: 5'-GCTGGCCACCTGCTGTC-3'; GAPDH Forward: 5'-GTCTCCTCTGACTTCAACAGCG-3', GAPDH Reverse: 5'-ACCACCCTGTTGCTGTAGCCAA-3'.

Western blot. Cells were lysed using the RIPA lysis solution (Boster, China, AR0102). Following heat-induced denaturation of the proteins, they were separated using SDS-PAGE and subsequently placed onto PVDF membranes (Millipore, USA). First, proteins were blocked for 1 h at room temperature using 5% non-fat milk. Next, primary antibodies, such as MTHFD2 (#A10386, ABclonal) and GAPDH (#A19056, ABclonal), were incubated overnight at 4 °C. Finally, the IgG-HRP secondary antibody was incubated for 2.5 h at room temperature. Following the addition of ECL chemiluminescent substrate (Boster, China), bands were seen using a ChemiDoc-It Imaging System (UVP, USA). ImageJ software (the National Institutes of Health; Bethesda, MD, USA) [16] was used to quantify band densities.

Construction of MTHFD2 silenced and overexpressing cell line. With the aid of the enzymes XBaI and BamHI (NEB), the sequence comprising MTHFD2 CDS (transcript NM_001410192) with restriction sites was cloned into the lentiviral vector pCDH-CMV-MCS-EF1-Puro (System Biosciences). shRNA sequences targeting MTHFD2 were designed using the shRNA design tool from Thermo Fisher (https://rnaidesigner.thermofisher.com/rnaiexpress/insert.do) and cloned into the pLKO.1-puro vector (Addgene). X-tremeGENE HP DNA Transfection Reagent (Roche) was used to co-transfect recombinant plasmids, packaging plasmid Δ8.91, and envelope plasmid pVSV-G into 293T

cells. Forty-eight hours after transfection, supernatants were collected, filtered, and then utilized to infect MCF-7 and MDA-MB-231 cells with polybrene. After 72 h, cells were treated with puromycin for 7–9 days. The effectiveness of MTHFD2 overexpression and silencing was confirmed by western blot and qRT-PCR.

Cell viability assay. The Cell Counting Kit-8 (CCK-8) test (Dojindo, Japan) was used to evaluate cell proliferation. In a 96-well plate with 2×10^3 cells/well, the cells were incubated for 0, 1, 2, and 3 days. 10 μl of CCK-8 solution was added each time, and the plate was incubated for 2 h at 37 °C. A microplate reader (CMax Plus, Molecular Devices, USA) was used to detect absorbance at 450 nm.

EdU proliferation assay. The EdU kit (Servicebio, G1603, China) was used to perform the EdU proliferation assay. Following the manufacturer's instructions, EdU incorporation and detection were carried out after 48 h of culture for breast cancer cells. Leica DM500 fluorescence microscope and Image-Pro Plus 6.0 software (VTl-IPP, version 6.0, MediaCybernetics Corporation, USA) were used to quantify fluorescence.

Cell cycle detection. Cells were fixed with 70% ethanol at –20 °C for 12 h after being treated with 0.25% trypsin. They were then collected and washed with PBS. Subsequently, 50 μg/ml propidium iodide (PI) was added to the cells, and they were exposed to 100 μg/ml RNase (both from Sigma-Aldrich) for two hours. ABI, USA's Attune flow cytometry was used to analyze the cell cycle distribution, and FlowJo V10 software was employed.

Analysis of potential pathways downstream of MTHFD2. Gene expression data from acute myeloid leukemia (GSE81062), bladder cancer (GSE217785), and human aortic endothelial cells (GSE100261) were collected from the Gene Expression Omnibus (GEO) database (https://www.ncbi.nlm.nih.gov/geo/) [17] to identify common genes downregulated after MTHFD2 silencing. Transcriptomic data from breast cancer were analyzed using the Cancer Genome Atlas and R software, with low-expression genes removed for quality assurance. Pearson correlation coefficients calculated the relationships between MTHFD2 and other genes, aiding in selecting KEGG pathways for Gene Set Enrichment Analysis (GSEA) [18]. Venn diagrams identified genes associated with MTHFD2, focusing on IFRD1 and its connection to the mTORC pathway.

IFRD1 RNA methylation analysis. Quantitative m6A methylation analysis of IFRD1 involved incubating 10 μg of RNA with 5 μg of m6A-specific antibody (68055-1-Ig) from Proteintech or control IgG. Following incubation with protein A/G beads, the RNA was isolated and quantified by qRT-PCR to assess IFRD1 enrichment.

Transfection and grouping. Cells were transfected with 100 nM of IFRD1 siRNA or siNC using Lipofectamine RNAiMAX, with efficiency assessed via qPCR and western blot 48 h later. Cells were grouped as follows: OE-NC (Overexpression Negative Control), OE-MTHFD2 (Overexpression of MTHFD2), MTHFD2+si-NC (cells were transfected with si-NC, and MTHFD2-overexpressed) MTHFD2+si-IFRD1 (MTHFD2-overexpressing cells were transfected with si-IRFD1) for subsequent assays, including CCK-8, EdU, and cell cycle analysis.

Chemosensitivity of MTHFD2-silenced cells. Breast cancer cells with MTHFD2 silenced were treated with doxorubicin (DOX), docetaxel (DTX), paclitaxel (PTX), capecitabine (Cape), and tamoxifen (TMX). Cell viability changes were evaluated using the CCK-8 assay 48 h post-treatment.

In addition, the drug sensitivity of MDA-MB-231 and MCF-7 cells to MTHFD2 inhibitor DS18561882 (DS) [19] was observed, and the IC50 value was calculated. Then DS18561882 was combined with classical chemotherapy drugs for 48 h to observe cell activity changes. The IC50 concentration value is used as the working concentration of the above-mentioned drugs.

The tumor-bearing experiment in nude mice. MDA-MB-231 cells (5×10^6) of negative control and MTHFD2-silenced MDA-MB-231 cells were injected subcutaneously into the breast fat pad of 6-week-old female nude mice with a body weight of 21±1 g. Animal groups: 1. sh-NC group (MDA-MB-231 cells infected with sh-NC, n=6); 2. sh-MTHFD2 group (MDA-MB-231 cells silenced by MTHFD2, n=6). Tumor volume was measured every five days post-injection. After 20 days of injection, the nude mice were euthanized by CO_2 asphyxiation. The tumor tissue was fixed in 4% paraformaldehyde, and paraffin embedding was performed. The expression level of MTHFD2, IFRD1, HDAC3, p-HDAC3, p53, acetylated p53, mTOR, mTOR, p-p70S6K, p-4EBP1 protein was detected by western blotting in tumor tissues (n=3). Animal experiments were approved by the Animal Ethics Committee of Dalian Medical University (Ethics number AEE23077).

Statistical analysis. The three separate experiments' means and standard deviations are shown in the data. Statistical significance was determined using t-tests or ANOVA with post-hoc tests when comparing multiple groups. GraphPad Prism 8.0 (GraphPad Software, USA. www.graphpad.com) was used for statistical analysis and graphing.

Results

Silencing and overexpression of MTHFD2 in breast cancer cells. To explore the biological function of MTHFD2 in breast cancer progression, we first analyzed the association between the expression level of MTHFD2 and breast cancer in clinical analysis. Firstly, immunohistochemical detection was conducted in the samples of breast cancer patients received by our hospital (Figure 1A), and it was found that the expression level of MTHFD2 protein in breast cancer tissues was significantly higher than that in adjacent tissues (Table 1). To deepen the relationship between MTHFD2 and malignant lesions of breast cancer, the expression level of MTHFD2

protein and clinicopathological factors were statistically analyzed. The results showed that the expression intensity of MTHFD2 was significantly correlated with tumor grade (p=0.034), lymph node metastasis (p=0.037), and recurrence level (p=0.032; Table 2). Moreover, TCGA database of breast cancer patients also showed that patients with high expression of the MTHFD2 gene had a worse prognosis (p=0.0018, Figure 1B). According to the ENCORI database's gene expression data, breast cancer tissues had a significantly higher level of MTHFD2 than normal breast tissues (Figure 1C). The results of the quantitative analysis demonstrated that the levels of MTHFD2 mRNA (Figure 1D) and protein (Figures 1E–F) in breast cancer cell lines MCF-7, MDA-MB-231, and MDA-MB-468 were significantly greater than those in normal breast epithelial cells (HMEC and Du4475), with statistical significance (p<0.01). To further explore the function of MTHFD2, we performed overexpression and silencing experiments using lentiviral vectors in MCF-7 and MDA-MB-231 cells. Successful overexpression and silencing were confirmed at both the gene (Figures 1G–H) and protein levels (Figures 1I–K, compared to controls, p<0.01).

MTHFD2 modulation influenced cell proliferation and cell cycle. MTHFD2 has a unique localization in the nucleus, possibly related to cell proliferation and cycle. Therefore, this section will detect changes in proliferation-related ability by constructing breast cancer cells that silence and overexpress MTHFD2. The influence of MTHFD2 modulation on cell proliferation was analyzed using CCK-8 (Figures 2A–B) and EdU assays (Figures 2C–E) in MCF-7 and MDA-MB-231 breast cancer cells. Overexpression of MTHFD2 significantly enhanced cell proliferation, which was evident from the upward trends in the CCK-8 assay curves (Figures 2A–B) and an increased percentage of EdU-positive cells (Figures 2C–E). These results, compared to the overexpression negative control (OE-NC) group, were statistically significant (p<0.05). Conversely, silencing MTHFD2 showed a marked reduction in proliferation, with lower curves in the CCK-8 assay and fewer EdU-positive cells, demonstrating significant inhibition compared to the silencing negative control (sh-NC) group (p<0.01). MTHFD2 overexpression enhanced the percentage of cells in the S+G2/M phase (Figures 2F–H), indicating facilitation of cell cycle progression, according to further cell cycle analysis by flow cytometry. On the contrary, silencing MTHFD2 reduced the proportion of cells in the S+G2/M phase, indicative of a potential delay or arrest in the cell cycle. These findings were statistically significant (p<0.01) and confirmed the critical role of MTHFD2 in cell cycle regulation.

Table 1. Immunohistochemical quantification of MTHFD2 protein.

Histological type	MTHFD2, n (%)					
	Num	-	+	++	+++	p-value
Breast cancer tissue	51	16 (31.4)	12 (23.5)	13 (25.5)	10 (19.6)	0.0024**
Para-carcinoma tissue	51	31 (60.8)	8 (15.7)	9 (17.6)	3 (5.9)	

Note: **p < 0.01, the difference was statistically significant

Table 2. Analysis of MTHFD2 expression intensity and clinicopathological factors of breast cancer.

Clinicopathological characteristics	**MTHFD2, n (%)**				
	–	+	++	+++	**p-value**
Age (years)					
≤40	10 (19.6)	3 (5.9)	4 (7.8)	2 (3.9)	0.24
>40	21 (41.2)	5 (9.8)	5 (9.8)	1 (2.0)	
Diameter of tumor (cm)					
≤1	16 (31.4)	3 (5.9)	5 (9.8)	1 (2.0)	
1–2	12 (23.5)	4 (7.8)	2 (3.9)	2 (3.9)	0.672
>3	3 (5.9)	1 (2.0)	2 (3.9)	0 (0)	
Tumor size					
1	3 (5.9)	1 (2.0)	2 (3.9)	0 (0)	
2	12 (23.5)	4 (7.8)	2 (3.9)	2 (3.9)	0.034*
3	10 (19.6)	3 (5.9)	5 (9.8)	1 (2.0)	
Lymphatic metastasis					
No	17 (33.3)	2 (3.9)	3 (5.9)	0 (0)	0.037*
Yes	14 (27.5)	6 (11.8)	6 (11.8)	3 (5.9)	
Relapse					
No	11 (21.6)	0 (0)	1 (2.0)	0 (0)	0.032*
Yes	20 (39.2)	8 (15.7	8 (15.7)	3 (5.9)	

Note: *p<0.01, the difference was statistically significant

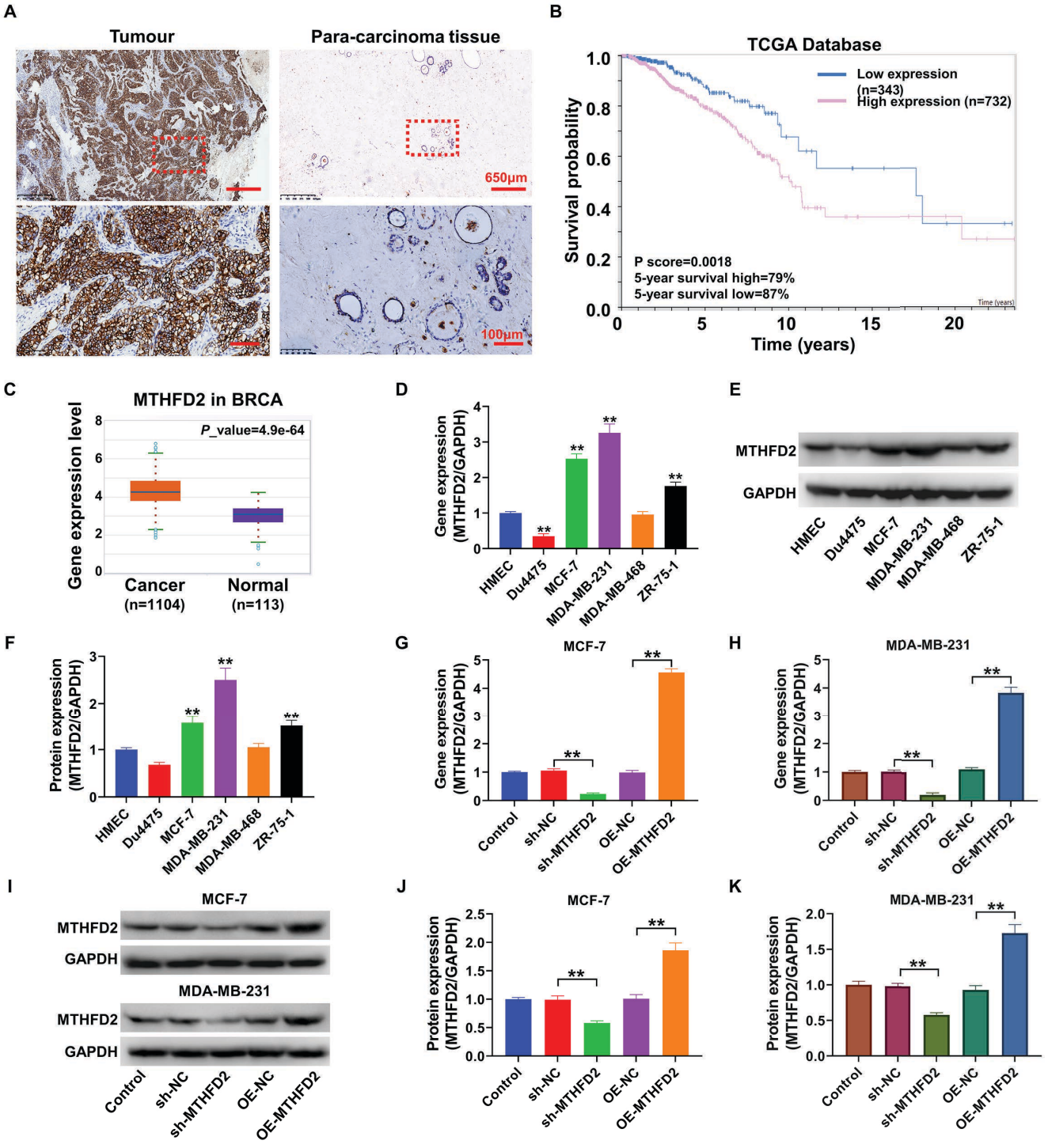

Figure 1. Construction of breast cancer cell lines with silenced and overexpressed MTHFD2. A) The expression levels of MTHFD2 protein in breast cancer tissue and adjacent tissues were analyzed by immunohistochemistry, and the image scales are 650 and 100 μm, respectively. The lower image is the enlarged image of the red box of the upper image. B) Survival analysis diagram between MTHFD2 expression intensity and prognosis level of breast cancer patients in ProteinAtlas database. MTHFD2 gene expression and prognosis data of patients were derived from TCGA database. C) The ENCORI database was used to analyze the differences in MTHFD2 gene expression between breast cancer patients and healthy persons. D) MTHFD2 gene expression levels in breast cancer cells and normal breast epithelial cell lines were detected using qRT-PCR. E, F) Results of protein band densitometry measurements on a western blot showing the levels of MTHFD2 protein expression. G, H) qRT-PCR detected MTHFD2 gene overexpression and silencing efficiency in cells. I–K) Western blot analysis of MTHFD2 protein overexpression and silencing efficiency in cells, with quantification of protein band densitometry values. **p<0.01, comparison between groups, indicating statistically significant differences

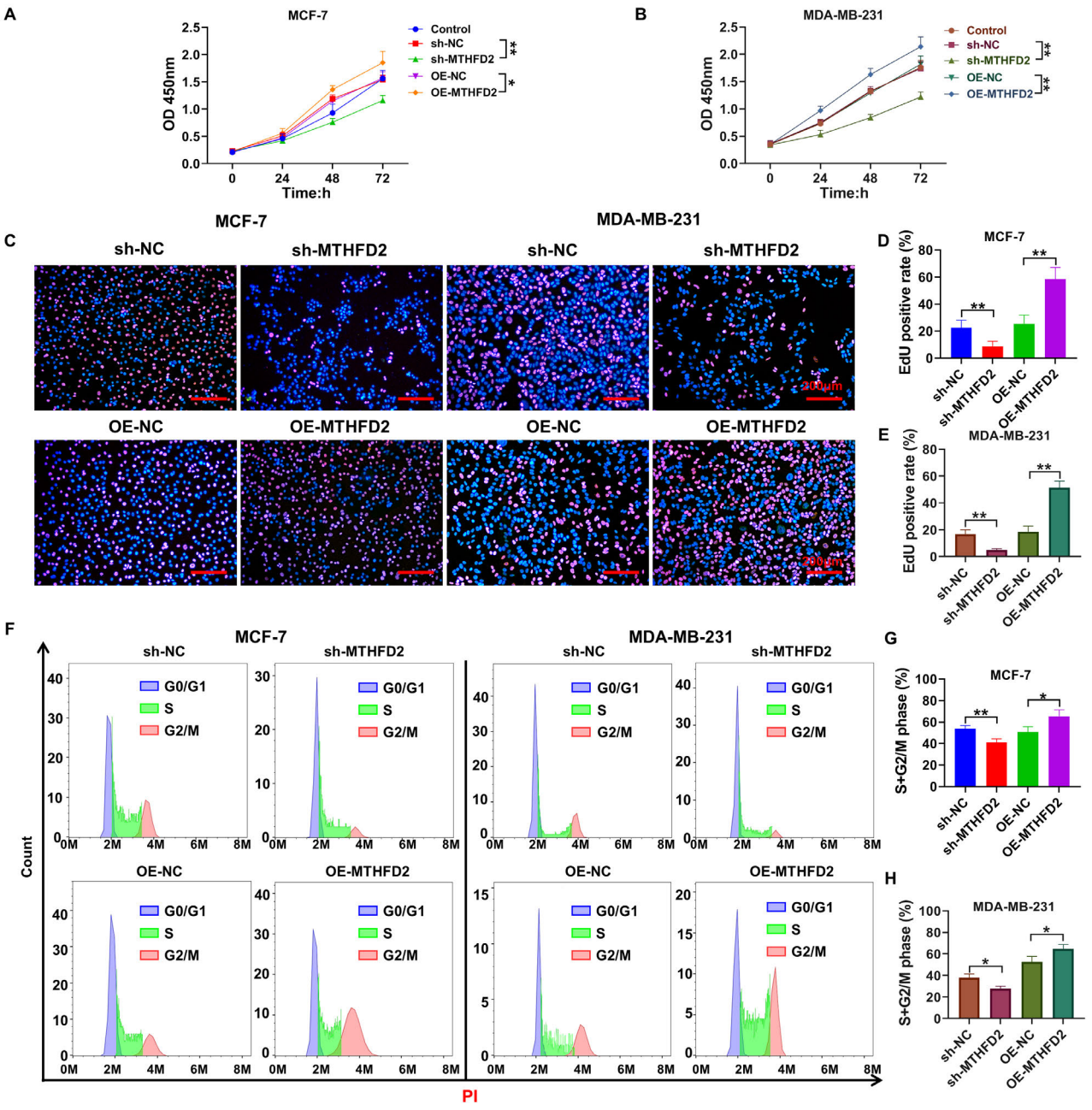

Figure 2. The effect of MTHFD2 on proliferation and cell cycle levels of breast cancer cells. A, B) CCK-8 assay to detect changes in cell viability. C–E) EdU staining is used to detect cells in the proliferative cycle, and the proportion of EdU-positive cells is analyzed using IPP6.0 software. F–H) Flow cytometry to detect changes in the cell cycle. *p<0.05, **p<0.01, comparison between groups indicating statistically significant differences

MTHFD2 may influence breast cancer proliferation through IFRD1 modulation. This part will screen the key mechanisms in combination with bioinformatics and existing clinical breast cancer databases to explain the mechanism of MTHFD2 differential expression in the abnormal proliferation of breast cancer cells. Analysis of gene expression changes following MTHFD2 silencing across various cancer types, including acute myeloid leukemia, bladder cancer, and aortic endothelial cells using the GEO database (Figure 3A), identified five consistently downregulated genes-NXN, RGS3, LFNG, C20orf27, and IFRD1. Subsequent correlation analysis using the GEPIA database highlighted a significant positive relationship between MTHFD2 and IFRD1 expression (p-value <0.000, R=0.46), suggesting a regulatory linkage (Figure 3B). Gene Set Enrichment Analysis (GSEA) showed that among MTHFD2-associated pathways, only IFRD1 is

involved in the mTOR cell growth pathway, underscoring its role in crucial cellular functions (Supplementary data S1). Validation through qRT-PCR (Figures 3C–D) and western blotting (Figures 3E–G) confirmed that MTHFD2 overexpression significantly increases IFRD1 gene and protein levels, whereas silencing MTHFD2 achieves the opposite effect, with both scenarios showing statistically significant differences ($p<0.01$). Furthermore, recognizing MTHFD2's potential to influence m6A methylation across various genes [20], we investigated its effect on the m6A methylation status of the IFRD1 gene methylation. RNA immunoprecipitation (Figures 3H–I) demonstrated that MTHFD2 silencing reduced m6A methylation of the IFRD1 gene, while overexpression enhanced it, marking significant epigenetic modifications that influence RNA stability and translation. These findings illustrate the profound impact of MTHFD2 on gene expression and cellular pathways, potentially offering new targets for therapeutic intervention.

MTHFD2 modulates cell proliferation through HDAC3 and mTOR phosphorylation. Bioinformatics and previous experimental results confirmed that MTHFD2 was positively correlated with the IFRD1 gene and protein. According to research reports, IFRD1 has been proven to have the effect of phosphorylating HDAC3 to deacetylate p53, thereby regulating the activation of mTOR protein. mTOR is a critical protein that regulates the abnormal proliferation of breast cancer cells. Therefore, activating this pathway has a positive significance in explaining that MTHFD2 promotes abnormal proliferation of breast cancer cells and increases the proportion of the G1/M phase. IFRD1 is known to modulate p53 acetylation through phosphorylated HDAC3, which in turn influences mTOR protein activation. The downstream effects of MTHFD2 on these regulatory proteins are investigated in this study using a western blot. Results shown in Figure 4 reveal that MTHFD2 overexpression significantly enhances the phosphorylation levels of HDAC3 and mTOR, leading to the activation of p70 S6K and 4EBP1, both critical regulators of cell proliferation. This upregulation is accompanied by a marked reduction in acetylated p53 and total protein levels, showing significant differences from the OE-NC group ($p<0.01$). In contrast, MTHFD2 silencing decreases the phosphorylation of HDAC3 and mTOR, curtailing the activation of p70 S6K and 4EBP1, and significantly increases the levels of acetylated p53 and total protein, compared to the OE-NC group ($p<0.01$).

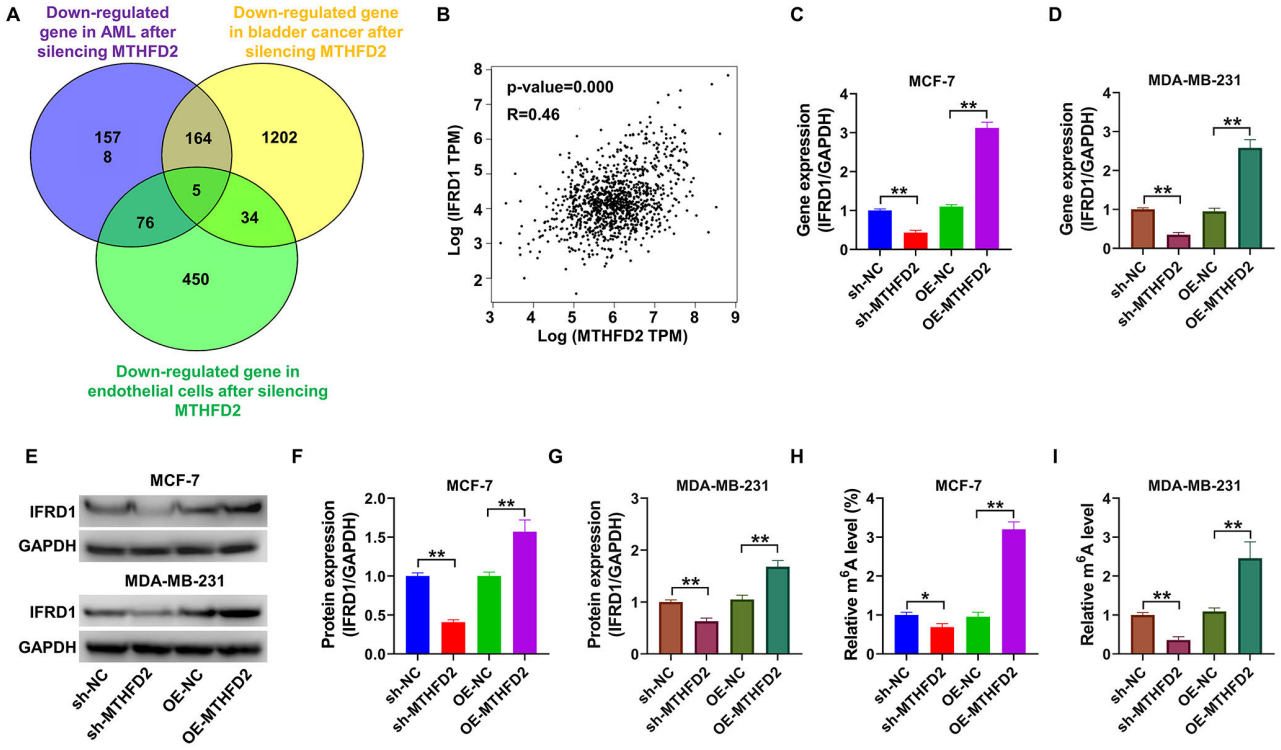

Figure 3. MTHFD2 influences the proliferation of breast cancer cells through IFRD1. A) Analysis of significantly downregulated genes after silencing MTHFD2 in three cell types using the GEO database, combined with a Venn diagram analysis. B) Examining the relationship between target genes and MTHFD2 expression in breast cancer by GEPIA database analysis. C, D) qRT-PCR detection of IFRD1 gene expression after overexpression and silencing of MTHFD2. E–G) Protein band densitometry values were quantified using a western blot analysis of IFRD1 protein expression after MTHFD2 overexpression and silencing. H, I) Detection of IFRD1 gene abundance after m6A methylation co-precipitation using qRT-PCR. **p<0.01, *p<0.05, comparison between groups indicating statistically significant differences

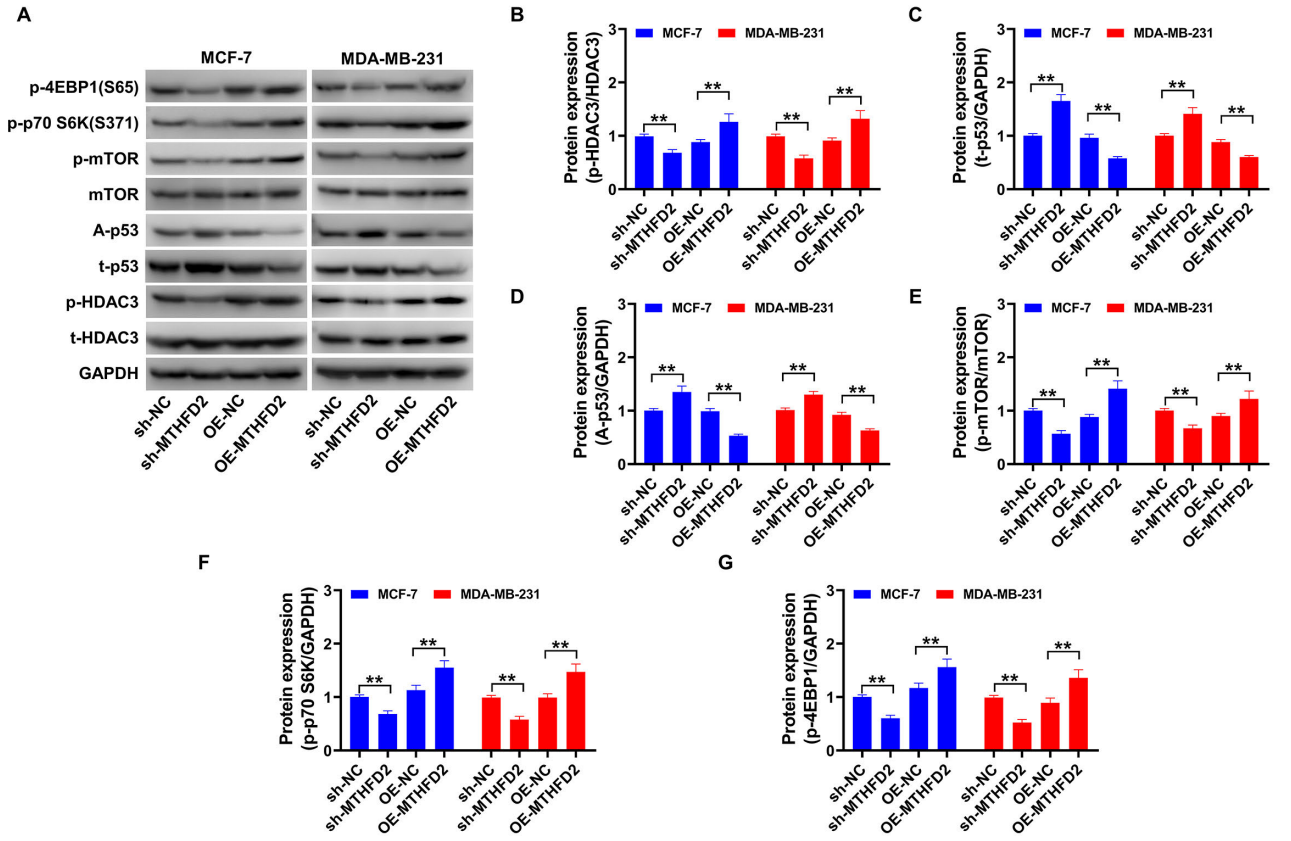

Figure 4. The effect of MTHFD2 on protein expression in downstream pathways, including IFRD1/p53/mTOR. A) The downstream regulatory proteins HDAC3/p-HDAC3/P53/acetyl-p53/mTOR/mTOR/p-p70S6K/p-4EBP1 can be detected by western blotting. B–G) Quantitative analysis of western blot band densitometry values. **p<0.01, comparison between groups indicating statistically significant differences

IFRD1 interference reverses the effect of MTHFD2 overexpression. While the expression of MTHFD2 is positively correlated with IFRD1 in breast cancer, its upstream and downstream relationship has not been clarified. Previously, it was only proved that silencing MTHFD2 can downregulate the IFRD1 gene and protein expression. To deepen the mechanism axial relationship, IFRD1 siRNA was introduced in this study for further verification. Western blot results confirmed that IFRD1 siRNA could significantly inhibit the expression of IFRD1 protein in MCF-7 and MDA-MB-231 cells but did not affect the expression of MTHFD2 protein (Figures 5A–C, p<0.01). This indicates that MTHFD2 expression is not affected by the IFRD1 protein. To prove that MTHFD2 induces abnormal proliferation of breast cancer cells through the upregulation of IFRD1, this part will conduct a rescue experiment by interfering with the expression of the IFRD1 protein. The results from the CCK-8 assay (Figures 5D–E) and EdU staining (Figures 5F–H) demonstrate that IFRD1 oligonucleotide transfection significantly counteracts the proliferative boost and increased EdU-positive cell rates induced by MTHFD2 overexpression in breast cancer cells. These effects show statistically significant differences in comparison with the MTHFD2+si-NC group (p<0.05). Furthermore, IFRD1 transfection notably reverses the increased S+G2/M phase proportion in breast cancer cells caused by MTHFD2 overexpression, with significant statistical differences (p<0.01, Figures 5I–K). In conclusion, MTHFD2 can promote the progression of breast cancer cells by inducing abnormal cell proliferation and abnormal increase of S+G2/M cell proportion thr oughIFRD1.

Impact of IFRD1 interference on MTHFD2-regulated pathways. To further verify that MTHFD2 regulates p53/mTOR and other downstream pathways through the upregulation of IFRD1, this part will conduct mechanism research by interfering with the expression of the IFRD1 protein rescue experiment. Overexpression of MTHFD2 markedly enhances the phosphorylation levels of HDAC3 and mTOR proteins, activating downstream cell proliferation regulators p70 S6K and 4EBP1 (Figure 6). This overexpression also substantially reduces the levels of acetylated p53 and total proteins, all with significant differences compared to the OE-NC group (p<0.01). Transfection of breast cancer cells overexpressing MTHFD2 with IFRD1 siRNA oligonucleotides significantly reversed the effects on these protein

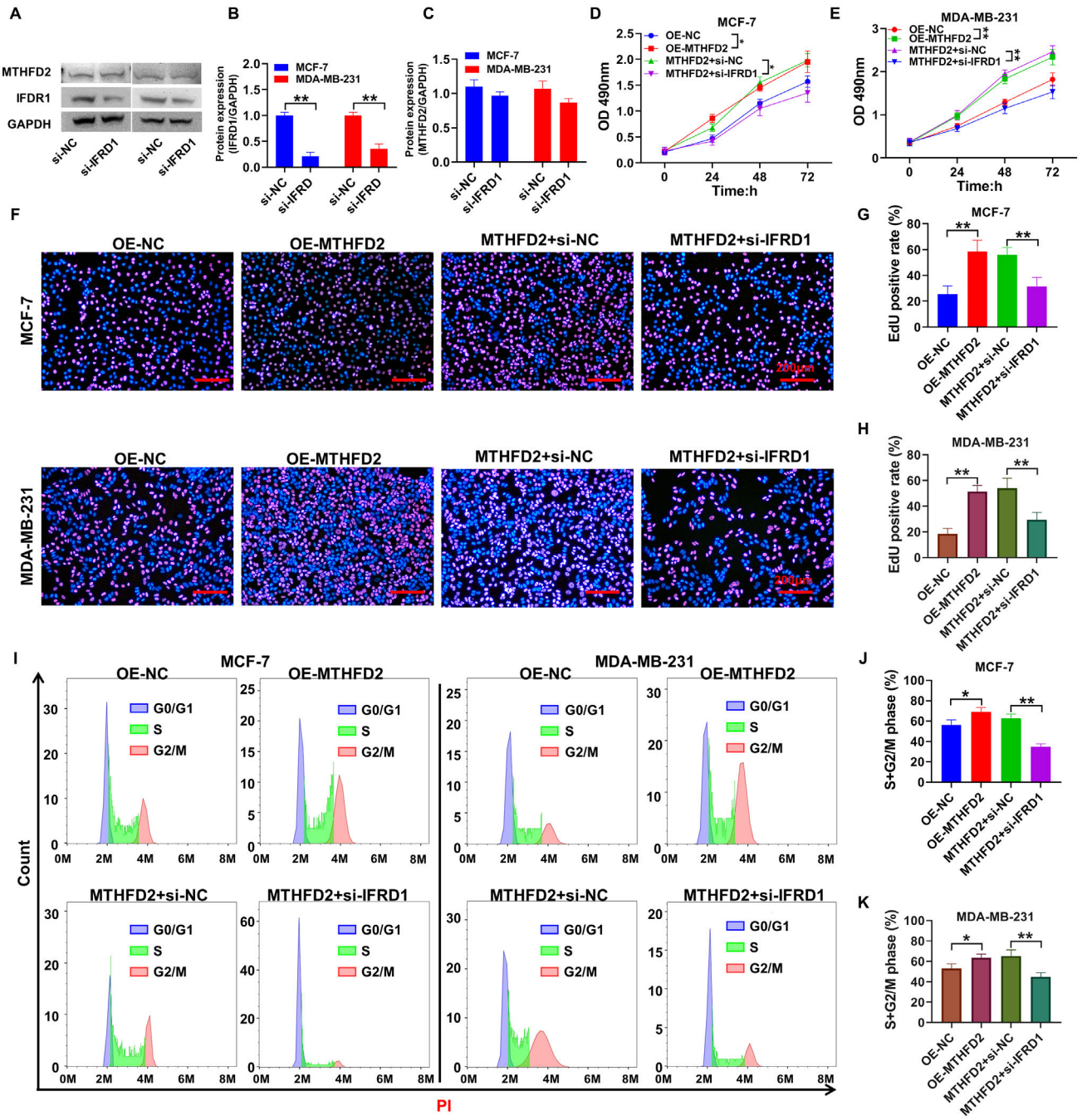

Figure 5. The effect of MTHFD2 overexpression on breast cancer growth is reversed by interfering with IFRD1. A–C) The effect of western blotting on the expression of IFRD1 and MTHFD2 proteins by IFRD1 siRNA. D, E) CCK-8 assay to detect changes in cell viability. F–H) EdU staining is used to detect cells in the proliferative phase, and the fraction of EdU-positive cells is calculated using the IPP6.0 program. I–K) Flow cytometry analysis of changes in the cell cycle. *p<0.05, **p<0.01, statistically significant differences between groups

expressions, with differences being statistically significant in comparison with the MTHFD2+si-NC group (p<0.01).

Enhanced chemosensitivity following MTHFD2 silencing. To identify MTHFD2 as a potential value target in treating breast cancer, we explored the sensitivity of silencing MTHFD2 to chemotherapy drugs combined with a variety of commonly used chemotherapy drugs. For the ultimate purpose of clinical treatment, a collaborative study was conducted with the typical inhibitor DS of MTHFD2 [19]. Drug sensitivity assays were performed using the CCK-8

method, testing sh-NC and sh-MTHFD2 cells with varying concentrations of classic chemotherapeutic agents: doxorubicin, docetaxel, paclitaxel, tamoxifen, and capecitabine. Results indicated that silencing MTHFD2 in MCF-7 cells significantly reduced the IC50 values for doxorubicin, docetaxel, paclitaxel, tamoxifen, and capecitabine from 718.0 nM, 80.95 nM, 645.30 nM, 113.50 nM, and 906.30 nM to 26.27 nM, 4.04nM, 15.98 nM, 40.83 nM, and 93.51 nM, respectively (Figures 7A–E). After silencing MTHFD2 in MDA-MB-231 cells, the IC50 values for doxorubicin, docetaxel, paclitaxel, tamoxifen, and capecitabine decreased from 199.7 nM, 1.26 μM, 1.13 μM, 8.96 μM, and 3.98 μM to 3.52 nM, 10.16 nM, 312.20 nM, 3.60 μM, and 0.84 μM, respectively. This indicates enhanced chemosensitivity of the breast cancer cells when MTHFD2 is silenced (Figures 7F–J). The semi-inhibitory rates of MTHDF2 inhibitor DS on MCF-7 or MDA-MB-231 cells were 1357 and 492 nM, respectively (Figure 7K), and the breast cells were treated with 1.3 or 0.5 μM DS in combination with the above chemotherapeutic drug IC50 for 48 h. The results showed that DS could significantly upregulate the inhibition rate of doxorubicin, docetaxel, paclitaxel, tamoxifen, and capecitabine on breast cancer cells, and the differences were statistically significant compared with the chemotherapy drug group alone (Figures 7K–L). In conclusion, silencing MTHFD2 or DS can significantly enhance the inhibition rate of breast cancer with chemotherapy drugs.

Silencing MTHFD2 inhibited tumor progression and affected MTHFD2/IFRD1/HDAC3/p53/mTOR pathway protein expression in nude mice with breast cancer. The inhibitory effect of silencing MTHFD2 on the proliferation of breast cancer cells has been demonstrated, but the environment of tumor tissue is often complex and variable. Therefore, to verify MTHFD2 as a potential target for breast cancer tumors, the efficacy and pathway were verified by transplantation of MDA-MB-231 cells silenced by MTHFD2 in nude mice in this study. According to the analysis of the tumor graph (Figure 8A) and volume growth trend graph (Figure 8B), silencing MTHFD2 could significantly inhibit tumor volume growth rate and size, and the difference was statistically significant compared with the sh-NC group ($p<0.01$). At the protein level, the silencing of MTHFD2 can significantly downregulate the expression of MTHFD2/

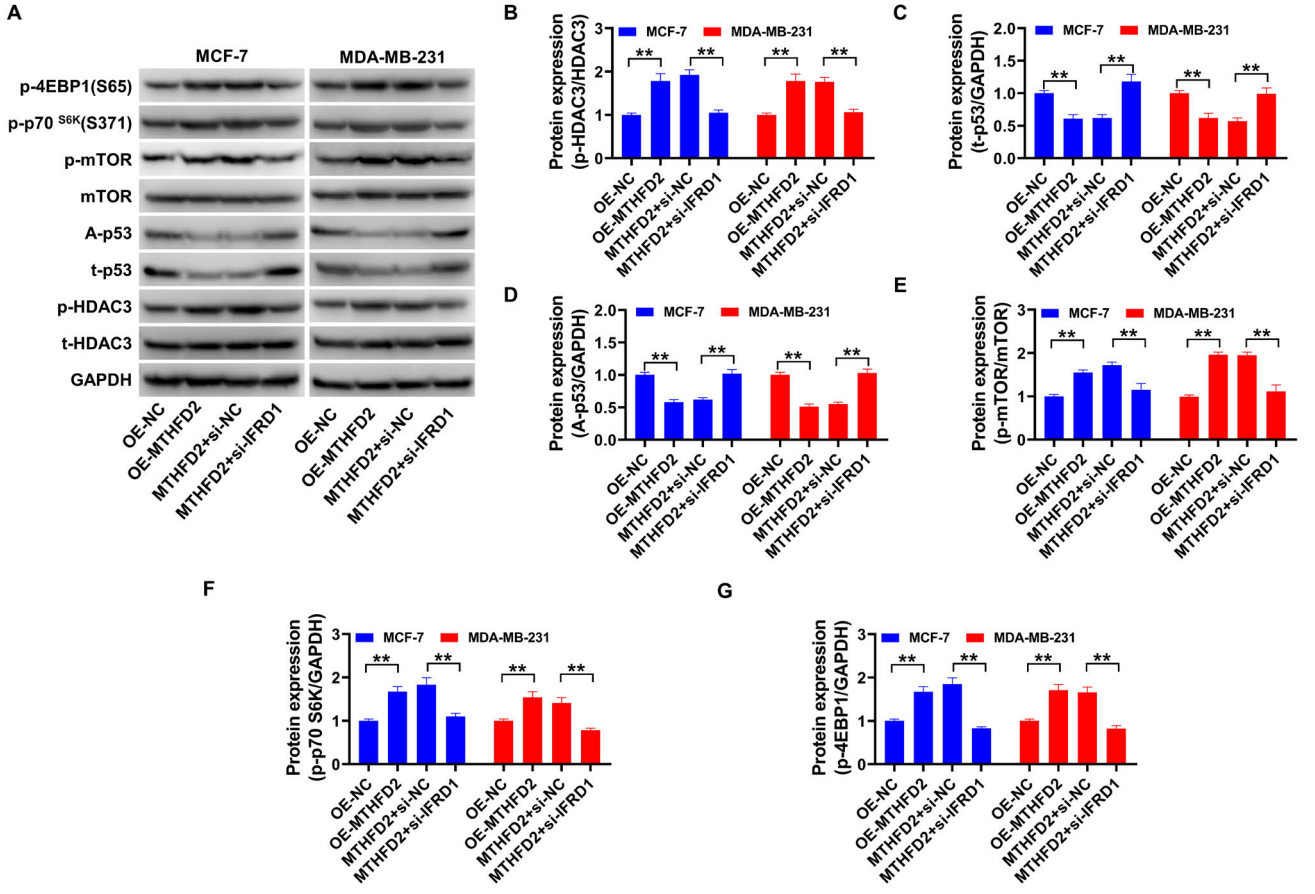

Figure 6. Effect of interfering with IFRD1 on the protein expression of downstream pathways regulated by MTHFD2 such as p53/mTOR. A) Western blotting to detect the expression changes of downstream regulatory proteins HDAC3/p-HDAC3/P53/acetyl-p53/mTOR/mTOR/p-p70 S6K/p-4EBP1. B–G) Quantitative analysis of western blot band densitometry values. **p<0.01, statistically significant differences between groups

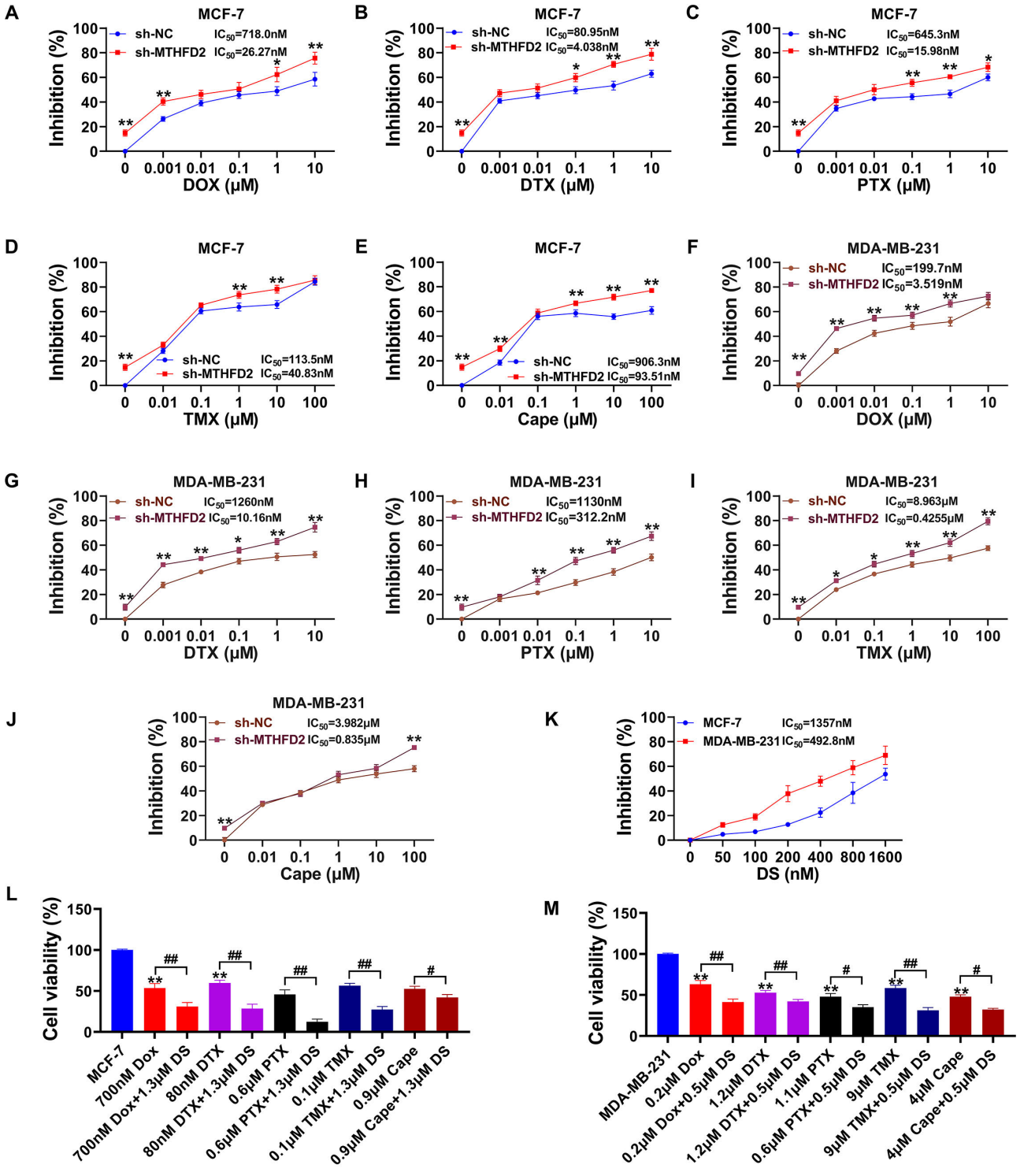

Figure 7. The effect of suppressing MTHFD2 in conjunction with different chemotherapeutic agents on the viability of breast cancer cells. A–E) CCK-8 assay to evaluate the effects of chemotherapeutic drugs, including doxorubicin, docetaxel, paclitaxel, tamoxifen, and capecitabine on the viability of MTHFD2-silenced and negative control MCF-7 cells. F–J) CCK-8 assay to assess the effects of chemotherapeutic drugs, including doxorubicin, docetaxel, paclitaxel, tamoxifen, and capecitabine, on the viability of MTHFD2-silenced and negative control MDA-MB-231 cells. K) CCK-8 detected the IC50 value of MTHFD2 classical inhibitor DS against MCF-7 and MDA-MB-231 cells. L, M) CCK-8 was used to detect the effect of DS combined with chemotherapeutic drugs on the activity levels of MCF-7 and MDA-MB-231 cells at IC50 concentration. **p<0.01, *p<0.05, the difference between sh-NC group and sh-MTHFD2 group was statistically significant at the same concentration

IFRD1/p-HDAC3/p-mTOR/p-p70 S6K/p-4EBP1 protein in tumor tissues and increase the expression level of t-p53/A-p53 protein. Compared with the sh-NC group, the expression level of MTHFD2/IFRD1/p-HDAC3/p-mTor/p-p70 S6K/p-4EBP1 protein can be improved. The differences were statistically significant ($p<0.01$, Figures 8C–E), providing robust evidence for the efficacy of silencing MTHFD2.

Discussion

High MTHFD2 expression is frequently linked to poor outcomes in breast cancer. Several studies have confirmed that reduced MTHFD2 expression can significantly impede breast cancer progression [5, 6]. Our study corroborates these findings and highlights MTHFD2 as a crucial regulator of the cell cycle and the proliferation of cancer cells. Previous investigations have explored various mechanisms of MTHFD2 in cancer; however, its specific roles in cell cycle regulation and nuclear localization remain undocumented. This study contributes to this gap by demonstrating how MTHFD2 overexpression and silencing affect breast cancer cells' proliferation and cell cycle progression, particularly influencing the G2/M phase – a critical phase for cell malignancy and proliferation [21].

To extend our understanding of MTHFD2's influence, we explored genes consistently downregulated across different cancers after MTHFD2 silencing by analyzing three GEO datasets (including acute myeloid leukemia, bladder cancer, and endothelial cells). This approach, despite the apparent lack of direct connection to breast cancer, provides a broader

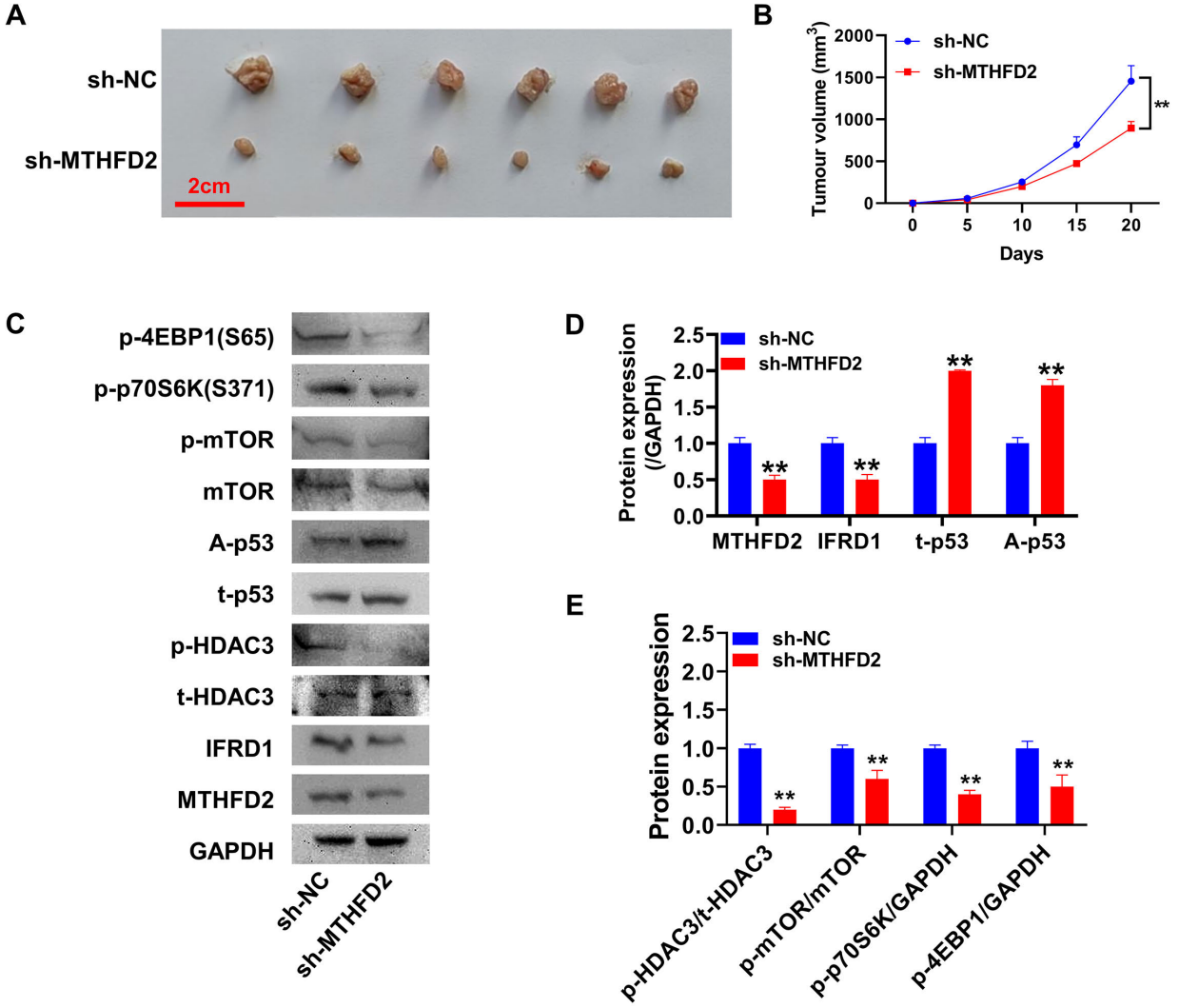

Figure 8. The effect of MTHFD2 on the expression of MTHFD2/IFRD1/HDAC3 p53/mTOR pathway protein in nude mice with breast cancer tumor. A) Tumor appearance in nude mice with tumor. B) Tumor growth trend in vivo of tumor-bearing nude mice; The expression level of MTHFD2/IFRD1/p-HDAC3/p-mTOR/p-p70 S6K/p-4EBP1/t-p53/A-p53 protein was detected by C-E) western blot, and the optical density of protein bands was quantitatively analyzed by ImageJ. **p<0.01, the difference between groups was statistically significant

genetic context, underscoring the generalizability and potential universal role of MTHFD2-regulated pathways. Our findings identify IFRD1 as a critical gene downregulated following MTHFD2 silencing, with further validation using the GEPIA database indicating a strong positive correlation between MTHFD2 and IFRD1. Notably, IFRD1 is involved in the mTOR pathway, known for its pivotal role in cancer growth and metabolism, marking it as the only significantly impacted pathway in our Hallmark analysis.

High expression of IFRD1 in breast cancer is associated with a worse prognosis (data collected from http://kmplot.com/analysis, the Kaplan-Meier Plotter database). The modulation of IFRD1 by MTHFD2 may thus represent a key mechanism in the progression of breast cancer. Our study confirms that overexpression of MTHFD2 correlates with increased IFRD1 gene and protein levels in breast cancer, whereas silencing MTHFD2 has the opposite effect, suggesting a regulatory relationship between MTHFD2 and IFRD1. Further insights into MTHFD2's role are provided by Nathanael et al. [20], who observed that MTHFD2 influences RNA methylation to stabilize HIF1α expression. Moreover, MTHFD2 has been implicated in promoting DNA methylation and functional inhibition of mTOR through these mechanisms [22–25]. In eukaryotes, m6A methylation predominantly occurs within the nucleus, specifically during the transcription of mRNA, which is the most common modification of mRNA methylation. It is involved in almost all stages of RNA processing, including regulation of mRNA transcription, maturation, translation, degradation, and stability [26, 27]. The function of MTHFD2 in regulating gene methylation aligns with previous reports of its localization in the cell nucleus, further demonstrating the feasibility of MTHFD2 in regulating the mTOR pathway. This study confirmed that MTHFD2 significantly increases IFRD1 mRNA methylation levels to stabilize IFRD1 mRNA through IFRD1 RNA methylation.

According to Garcia et al. [28], IFRD1 is a transcriptional co-activator/inhibitor that may control intestinal lipid metabolism and epithelial cell proliferation. In normal homeostasis, IFRD1 is expressed at low levels in a variety of organs and cell types; however, in many malignant tumors, such as colorectal adenocarcinoma, it is substantially expressed [29, 30]. By interacting with transcription factors or histone deacetylase complexes, IFRD1 can regulate the expression of specific genes [28, 31]. Prior studies have indicated that IFRD1 can phosphorylate or recruit histone deacetylase 3 (HDAC3) to carry out transcription factor deacetylation activities., mediating its protein degradation and thereby regulating the transcription of downstream genes [32, 33]. IFRD1 can inhibit p53 accumulation, enhance mTORC1 reactivation, and promote cell proliferation [34], while HDAC3 has been noted to affect the inactivation and stability of p53 protein, facilitating its downregulation and degradation [33, 35].

Of note, this study analyzed the critical pathways of MTHFD2 in breast cancer using GSEA-Hallmark, identifying the mTOR pathway as one of the critical pathways mediating abnormal proliferation in breast cancer. Activation of p53 can inhibit the activation of the mTOR pathway [36], thereby limiting the restraining of downstream cell cycle-related kinases p70 S6K and 4EBP1 while enhancing cell survival and proliferation abilities [37]. Additionally, IFRD1 has also been shown to regulate the deacetylation and subsequent degradation of p53 protein, weakening p53's inhibitory effect on mTOR and promoting cell proliferation [34].

Therefore, to determine that MTHFD2 regulates downstream pathways by stabilizing *IFRD1* gene expression, this study experimentally showed that interfering with *IFRD1* gene and protein expression significantly reversed the upregulation of HDAC3/mTOR protein phosphorylation levels induced by MTHFD2 overexpression. It also induced the activation of p70 S6K and 4EBP1 proteins, which are downstream regulators of mTOR involved in cell proliferation. Additionally, interfering with IFRD1 expression reversed the inhibitory effect of MTHFD2 overexpression on acetylated p53 protein and its total protein.

This study preliminarily elucidates the therapeutic value of MTHFD2 in breast cancer. We also explore combining classical chemotherapeutic drugs used in breast cancer treatment to translate these research findings into clinical applications. It was determined that silencing MTHFD2 in combination with chemotherapeutic drugs can amplify the efficacy of these drugs. This provides better treatment options for breast cancer patients in clinical practice. Furthermore, since breast cancer exhibits distinct molecular subtypes, treatment with specific targeted drugs is required. This study employed cell lines representing different phenotypes: MCF-7 cells, the ER and PR-positive phenotype, and MDA-MB-231 cells, the triple-negative breast cancer. To expand the scope of these research findings, subsequent investigations will involve additional cell lines with different phenotypes, particularly those resistant to certain chemotherapeutic drugs. The combined treatment efficacy will be observed, aiming to achieve targeted therapy for patients with different phenotypes in a clinical setting.

In summary, MTHFD2 can stabilize RNA and increase transcription and translation by promoting the methylation of IFRD1 RNA, thereby activating HDAC3 and inhibiting the activation of p53 through protein function. Furthermore, the inhibitory effect of p53 on the mTOR/p70 S6K/4EBP1 pathway is weakened, and the proliferation activity of breast cancer cells is up-regulated. In addition, by silencing MTHFD2 and inhibitors, breast cancer patients can enhance their sensitivity to chemotherapy drugs. Therefore, this study suggests that MTHFD2 is a valuable potential target for breast cancer treatment. In future clinical studies, the tumor inhibition effect of conventional breast cancer chemotherapy drugs is expected to be enhanced through synergistic MTHFD2 inhibitors.

Supplementary information is available in the online version of the paper.

Acknowledgments: This study was supported by a Science Grant to Miss Xiaotang Yu from the Department of Education, Liaoning Province (grant no. LJKZ0839) and The Key Laboratory of Tumor Stem Cell Research of Liaoning Province.

References

[1] SUNG H, FERLAY J, SIEGEL RL, LAVERSANNE M, SOERJOMATARAM I et al. Global Cancer Statistics 2020: GLOBOCAN Estimates of Incidence and Mortality Worldwide for 36 Cancers in 185 Countries. CA Cancer J Clin 2021; 71: 209–249. https://doi.org/10.3322/caac.21660

[2] XIU Y, FIELD MS. The Roles of Mitochondrial Folate Metabolism in Supporting Mitochondrial DNA Synthesis, Oxidative Phosphorylation, and Cellular Function. Curr Dev Nutr 2020; 4: nzaa153. https://doi.org/10.1093/cdn/nzaa153

[3] NILSSON R, JAIN M, MADHUSUDHAN N, SHEPPARD NG, STRITTMATTER L et al. Metabolic enzyme expression highlights a key role for MTHFD2 and the mitochondrial folate pathway in cancer. Nat Commun 2014; 5: 3128. https://doi.org/10.1038/ncomms4128

[4] LIU F, LIU Y, HE C, TAO L, HE X et al. Increased MTHFD2 expression is associated with poor prognosis in breast cancer. Tumour Biol 2014; 35: 8685–8690. https://doi.org/10.1007/s13277-014-2111-x

[5] HUANG J, QIN Y, LIN C, HUANG X, ZHANG F. MTHFD2 facilitates breast cancer cell proliferation via the AKT signaling pathway. Exp Ther Med 2021; 22: 703. https://doi.org/10.3892/etm.2021.10135

[6] LEHTINEN L, KETOLA K, MÄKELÄ R, MPINDI JP, VIITALA M et al. High-throughput RNAi screening for novel modulators of vimentin expression identifies MTHFD2 as a regulator of breast cancer cell migration and invasion. Oncotarget 2013; 4: 48–63. https://doi.org/10.18632/oncotarget.756

[7] ZHANG H, ZHU S, ZHOU H, LI R, XIA X et al. Identification of MTHFD2 as a prognostic biomarker and ferroptosis regulator in triple-negative breast cancer. Front Oncol 2023; 13: 1098357. https://doi.org/10.3389/fonc.2023.1098357

[8] ZHANG F, WANG D, LI J, SU Y, LIU S et al. Deacetylation of MTHFD2 by SIRT4 senses stress signal to inhibit cancer cell growth by remodeling folate metabolism. J Mol Cell Biol 2022; 14. https://doi.org/10.1093/jmcb/mjac020

[9] GUSTAFSSON SHEPPARD N, JARL L, MAHADESSIAN D, STRITTMATTER L, SCHMIDT A et al. The folate-coupled enzyme MTHFD2 is a nuclear protein and promotes cell proliferation. Sci Rep 2015; 5: 15029. https://doi.org/10.1038/srep15029

[10] HARE SH, HARVEY AJ. mTOR function and therapeutic targeting in breast cancer. Am J Cancer Res 2017; 7: 383.

[11] LI JH, LIU S, ZHOU H, QU LH, YANG JH. starBase v2.0: decoding miRNA-ceRNA, miRNA-ncRNA and protein-RNA interaction networks from large-scale CLIP-Seq data. Nucleic Acids Res 2014; 42: D92–97. https://doi.org/10.1093/nar/gkt1248

[12] SJSTEDT E, ZHONG W, FAGERBERG L, KARLSSON M, MITSIOS N et al. An atlas of the protein-coding genes in the human, pig, and mouse brain. Science 2020; 367: eaay5947. https://doi.org/10.1126/science.aay5947

[13] GAO ZJ, FANG Z, YUAN JP, SUN SR, LI B. Integrative multi-omics analyses unravel the immunological implication and prognostic significance of CXCL12 in breast cancer. Front Immunol 2023; 14: 1188351. https://doi.org/10.3389/fimmu.2023.1188351

[14] ZHOU Y, JIA Z, WANG J, HUANG S, YANG S et al. Curcumin reverses erastin-induced chondrocyte ferroptosis by upregulating Nrf2. Heliyon 2023; 9: e20163. https://doi.org/10.1016/j.heliyon.2023.e20163

[15] RAO X, HUANG X, ZHOU Z, LIN X. An improvement of the 2ˆ(–delta delta CT) method for quantitative real-time polymerase chain reaction data analysis. Biostat Bioinforma Biomath 2013; 3: 71–85.

[16] SCHNEIDER CA, RASBAND WS, ELICEIRI KW. NIH Image to ImageJ: 25 years of image analysis. Nat Methods 2012; 9: 671–675. https://doi.org/10.1038/nmeth.2089

[17] BARRETT T, WILHITE SE, LEDOUX P, EVANGELISTA C, KIM IF et al. NCBI GEO: archive for functional genomics data sets--update. Nucleic Acids Res 2013; 41: D991–995. https://doi.org/10.1093/nar/gks1193

[18] WANG B, VAN DER KLOET F, KES M, LUIRINK J, HAMOEN LW. Improving gene set enrichment analysis (GSEA) by using regulation directionality. Microbiol Spectr 2024; 12: e0345623. https://doi.org/10.1128/spectrum.03456-23

[19] KAWAI J, TOKI T, OTA M, INOUE H, TAKATA Y et al. Discovery of a Potent, Selective, and Orally Available MTHFD2 Inhibitor (DS18561882) with in Vivo Antitumor Activity. J Med Chem 2019; 62: 10204–10220. https://doi.org/10.1021/acs.jmedchem.9b01113

[20] GREEN NH, GALVAN DL, BADAL SS, CHANG BH, LEBLEU VS et al. MTHFD2 links RNA methylation to metabolic reprogramming in renal cell carcinoma. Oncogene 2019; 38: 6211–6225. https://doi.org/10.1038/s41388-019-0869-4

[21] OSHI M, TAKAHASHI H, TOKUMARU Y, YAN L, RASHID OM et al. G2M Cell Cycle Pathway Score as a Prognostic Biomarker of Metastasis in Estrogen Receptor (ER)-Positive Breast Cancer. Int J Mol Sci 2020; 21: 2921. https://doi.org/10.3390/ijms21082921

[22] DENG X, SU R, WENG H, HUANG H, LI Z et al. RNA N6-methyladenosine modification in cancers: current status and perspectives. Cell Res 2018; 28: 507–517. https://doi.org/10.1038/s41422-018-0034-6

[23] SUGIURA A, ANDREJEVA G, VOSS K, HEINTZMAN DR, XU X et al. MTHFD2 is a metabolic checkpoint controlling effector and regulatory T cell fate and function. Immunity 2022; 55: 65–81.e9. https://doi.org/10.1016/j.immuni.2021.10.011

[24] WANG S, CHAI P, JIA R, JIA R. Novel insights on m6A RNA methylation in tumorigenesis: a double-edged sword. Mol Cancer 2018; 17: 101. https://doi.org/10.1186/s12943-018-0847-4

[25] ZHENG G, DAHL JA, NIU Y, FEDORCSAK P, HUANG CM et al. ALKBH5 is a mammalian RNA demethylase that impacts RNA metabolism and mouse fertility. Mol Cell 2013; 49: 18–29. https://doi.org/10.1016/j.molcel.2012.10.015

[26] GU C, SHI X, DAI C, SHEN F, ROCCO G et al. RNA m6A Modification in Cancers: Molecular Mechanisms and Potential Clinical Applications. Innovation (Camb) 2020; 1: 100066. https://doi.org/10.1016/j.xinn.2020.100066

[27] SUN T, WU R, MING L. The role of m6A RNA methylation in cancer. Biomed Pharmacother 2019; 112: 108613. https://doi.org/10.1016/j.biopha.2019.108613

[28] GARCIA AM, WAKEMAN D, LU J, ROWLEY C, GEISMAN T et al. Tis7 deletion reduces survival and induces intestinal anastomotic inflammation and obstruction in high-fat diet-fed mice with short bowel syndrome. Am J Physiol Gastrointest Liver Physiol 2014; 307: G642–654. https://doi.org/10.1152/ajpgi.00374.2013

[29] SABATES-BELLVER J, VAN DER FLIER LG, DE PALO M, CATTANEO E, MAAKE C et al. Transcriptome profile of human colorectal adenomas. Mol Cancer Res 2007; 5: 1263–1275. https://doi.org/10.1158/1541-7786.MCR-07-0267

[30] ZHANG B, WANG J, WANG X, ZHU J, LIU Q et al. Proteogenomic characterization of human colon and rectal cancer. Nature 2014; 513: 382–387. https://doi.org/10.1038/nature13438

[31] ONISHI Y, PARK G, IEZAKI T, HORIE T, KANAYAMA T et al. The transcriptional modulator Ifrd1 is a negative regulator of BMP-2-dependent osteoblastogenesis. Biochem Biophys Res Commun 2017; 482: 329–334. https://doi.org/10.1016/j.bbrc.2016.11.063

[32] MICHELI L, LEONARDI L, CONTI F, MARESCA G, COLAZINGARI S et al. PC4/Tis7/IFRD1 stimulates skeletal muscle regeneration and is involved in myoblast differentiation as a regulator of MyoD and NF-kappaB. J Biol Chem 2011; 286: 5691–5707. https://doi.org/10.1074/jbc.M110.162842

[33] TUMMERS B, GOEDEMANS R, PELASCINI LP, JORDANOVA ES, VAN ESCH EM et al. The interferon-related developmental regulator 1 is used by human papillomavirus to suppress NFκB activation. Nat Commun 2015; 6: 6537. https://doi.org/10.1038/ncomms7537

[34] MIAO ZF, LEWIS MA, CHO CJ, ADKINS-THREATS M, PARK D et al. A Dedicated Evolutionarily Conserved Molecular Network Licenses Differentiated Cells to Return to the Cell Cycle. Dev Cell 2020; 55: 178–194.e7. https://doi.org/10.1016/j.devcel.2020.07.005

[35] HE R, LIU B, GENG B, LI N, GENG Q. The role of HDAC3 and its inhibitors in regulation of oxidative stress and chronic diseases. Cell Death Discov 2023; 9: 131. https://doi.org/10.1038/s41420-023-01399-w

[36] MRAKOVCIC M, FRÖHLICH LF. p53-Mediated Molecular Control of Autophagy in Tumor Cells. Biomolecules 2018; 8: 14. https://doi.org/10.3390/biom8020014

[37] KARLSSON E, PÉREZ-TENORIO G, AMIN R, BOSTNER J, SKOOG L et al. The mTOR effectors 4EBP1 and S6K2 are frequently coexpressed, and associated with a poor prognosis and endocrine resistance in breast cancer: a retrospective study including patients from the randomised Stockholm tamoxifen trials. Breast Cancer Res 2013; 15: R96. https://doi.org/10.1186/bcr3557

https://doi.org/10.4149/neo_2024_240719N305

MTHFD2 promotes breast cancer cell proliferation through IFRD1 RNA m6A methylation-mediated HDAC3/p53/mTOR pathway

Qingqing ZHANG[1,#], Jun MAO[2,#], Luhan XIE[1,#], Ying LU[2], Xiaobo LI[1], Lianhong LI[1,*], Xiaotang YU[1,*]

Supplementary Information

Supplement 1 data

ID	setSize	pvalue	geneID
HALLMARK_E2F_TARGETS	199	7.79E-63	SMC4,CDK4,DDX39A,STAG1,CDKN2A,CDKN2C,CDKN3,TACC3,,SYNCRIP,IPO7,NOP56,PRDX4,PAICS,SPAG5,CENPE,RAD51AP1,CTCF,POLD3,PLK4,MTHFD2,KIF2C,NUDT21,CHEK1,CIT,PSIP1,CHEK2,CKS1B,CKS2,CSE1L,KIF18B,SPC24,CTPS1,DCK,DNMT1,EIF2S1,TUBB,AK2,EZH2,NUP205,CBX5,ORC6,KIF4A,MMS22L,XRCC6,ASF1A,UBE2S,ATAD2,UBE2T,RACGAP1,GSPT1,PSMC3IP,DONSON,H2AX,H2AZ1,HELLS,HMGB2,HMGB3,HMGA1,HMMR,HNRNPD,BIRC5,HUS1,ILF3,KIF22,KPNA2,STMN1,LBR,LIG1,LMNB1,MAD2L1,MCM2,MCM3,MCM4,MCM5,MCM6,MCM7,MKI67,MRE11,MSH2,MYBL2,MYC,NAP1L1,NASP,NBN,ORC2,PA2G4,PCNA,JPT1,PLK1,PMS2,PNN,POLD1,POLD2,POLE,ING3,TIPIN,PPP1R8,CDCA8,PRIM2,DEPDC1,LYAR,ASF1B,PRKDC,PRPS1,NUP107,SPC25,BARD1,RAD1,RAD21,RAD51C,RAN,RANBP1,RFC1,RFC2,RFC3,RPA1,RPA2,RRM2,SRSF1,SRSF2,TRA2B,GINS3,DCLRE1B,BRCA1,SSRP1,BRCA2,AURKA,SUV39H1,TCF19,BUB1B,TFRC,TK1,TMPO,TOP2A,TUBG1,UNG,USP1,WEE1,XPO1,SLBP,CENPM,DSCC1,DEK,SMC6,E2F8,ANP32E,DIAPH3,SMC1A,CDCA3,GINS4,BRMS1L,PHF5A,PPM1D,EED,TIMELESS,CCNE1,CNOT9,SMC3,CCNB2,ZW10,AURKB,NOLC1,PTTG1,TBRG4,TRIP13,ESPL1,CCP110,DLGAP5,CDK1,MELK,GINS1,CDC20,NCAPD2,CDC25A,CDC25B,NUP153
HALLMARK_G2M_CHECKPOINT	197	6.16E-55	TROAP,CHAF1A,SMC4,G3BP1,CDK4,DDX39A,STAG1,TRAIP,CDKN2C,CDKN3,NDC80,PRMT5,RBM14,TACC3,,SYNCRIP,CENPA,SMC2,CENPE,CENPF,CTCF,POLQ,PLK4,NUP50,SRSF10,DBF4,CBX1,KIF2C,TENT4A,UBE2C,KATNA1,CHEK1,CKS1B,CKS2,MAPK14,DKC1,DR1,DTYMK,E2F1,E2F2,E2F3,E2F4,EZH2,FANCC,MTF2,TPX2,ORC6,KIF4A,AMD1,FBXO5,UBE2S,RACGAP1,GSPT1,TNPO2,H2AX,H2AZ1,HIF1A,HMGB3,HMGN2,HMGA1,HMMR,HNRNPD,HNRNPU,HSPA8,BIRC5,HUS1,ILF3,INCENP,KIF5B,KIF11,KIF22,KPNB1,KPNA2,KMT5A,STMN1,LBR,LIG3,LMNB1,MAD2L1,MCM2,MCM3,MCM5,MCM6,MKI67,MYBL2,MYC,NASP,NCL,NEK2,NUP98,ODC1,ODF2,ORC5,JPT1,GINS2,PLK1,POLE,PRIM2,PBK,KIF15,KNL1,BARD1,RAD21,RAD23B,RBL1,SFPQ,SRSF1,SRSF2,TRA2B,STIL,SLC7A1,SMARCC1,SNRPD1,SQLE,BRCA2,AURKA,SUV39H1,BUB1,TFDP1,TMPO,TOP1,TOP2A,TTK,HIRA,UCK2,NSD2,XPO1,CUL5,SLC7A5,SMC1A,CDC7,CDC45,RAD54L,CUL4A,CUL3,CUL1,SAP30,PRPF4B,CCNA2,CCNF,CCNT1,CCNB2,EXO1,AURKB,NOLC1,PTTG1,H2AZ2,RASAL2,KIF23,KIF20B,ESPL1,CDK1,CDC6,CDC20,CDC25A,CDC25B,CDC27,CASP8AP2
HALLMARK_MYC_TARGETS_V1	198	2.82E-44	UBA2,G3BP1,CDK2,CDK4,PSMD14,HNRNPR,SF3A1,,SYNCRIP,NOP56,PRDX4,CCT7,CCT4,CCT2,PTGES3,YWHAQ,COPS6,PWP1,XPOT,PHB2,CBX3,CTPS1,CYC1,DHX15,EIF1AX,EIF2S1,EIF4E,EIF4G2,EPRS1,ETF1,HNRNPA3,NCBP2,CCT5,TARDBP,SF3B3,XRCC6,SERBP1,GNL3,PABPC1,GLO1,GSPT1,H2AZ1,HDAC2,HDGF,HNRNPA2B1,HNRNPC,HNRNPD,HNRNPU,HPRT1,HSP90AB1,HSPD1,IARS1,IFRD1,ILF2,KARS1,KPNB1,KPNA2,LDHA,MAD2L1,MCM2,MCM4,MCM5,MCM6,MCM7,MYC,NAP1L1,NCBP1,NPM1,ODC1,ORC2,PA2G4,HDDC2,PCNA,ACP1,PGK1,PHB1,SLC25A3,POLE3,POLD2,PPIA,PPM1G,PRPS2,PSMA4,PSMA7,PSMB2,STARD7,PSMC4,PSMD1,PSMD7,PSMD8,LSM2,RAD23B,RAN,RANBP1,RFC4,ABCE1,RRM1,SET,SRSF1,SRSF2,SRSF3,SRSF7,TRA2B,MRPL9,SMARCC1,SNRPA1,SNRPD1,SNRPD3,SNRPG,SRPK1,SSB,SSBP1,TCP1,TFDP1,C1QBP,CCT3,TYMS,UBE2E1,UBE2L3,USP1,VBP1,VDAC1,VDAC3,EIF4H,XPO1,YWHAE,CNBP,CAD,DEK,AIMP2,CANX,CDC45,CUL1,EIF3B,EIF3D,EIF3J,PABPC4,DDX18,EIF2S2,CCNA2,DDX21,NOLC1,COX5A,TOMM70,CDC20
HALLMARK_MTORC1_SIGNALING	197	9.43E-29	ACTR3,ACTR2,NAMPT,PSME3,DDX39A,PSMD14,TOMM40,POLR3G,YKT6,CTSC,MTHFD2,MLLT11,STIP1,COPS5,IMMT,PDAP1,STARD4,DDIT3,DHCR7,DHFR,ENO1,AK4,EPRS1,ETF1,NUP205,SEC11A,PITPNB,G6PD,SLC37A4,GAPDH,TES,PHGDH,GBE1,NUFIP1,DAPP1,CACYBP,SERP1,TMEM97,GOT1,GPI,TBK1,GSK3B,GSR,GTF2H1,PSAT1,ERO1A,HK2,HMGCR,HMGCS1,HPRT1,HSPA4,HSPA5,HSPA9,HSPD1,HSPE1,IDI1,IFRD1,INSIG1,LDHA,M6PR,MCM2,MCM4,ME1,ASNS,ACLY,NFIL3,NFYC,PNP,ATP2A2,P4HA1,PRDX1,UCHL5,PDK1,PFKL,PGK1,PGM1,PLK1,PLOD2,PPA1,PPIA,LGMN,PSMA3,PSMA4,PNO1,PSMB5,PSMC2,PSMC4,PSMC6,PSMD12,PSPH,TRIB3,BCAT1,RAB1A,RPA1,RPN1,RRM2,SCD,SHMT2,SLC1A5,SLC2A1,SQLE,SRD5A1,SSR1,AURKA,TCEA1,BUB1,TFRC,TPI1,HSP90B1,TUBG1,TXNRD1,UBE2D3,UNG,VLDLR,WARS1,ELOVL6,CYB5B,CALR,SLC7A5,ARPC5L,CANX,PIK3R3,USO1,PSMG1,GMPS,EIF2S2,CCNF,CCT6A,FADS2,EEF1E1,CDC25A
HALLMARK_MITOTIC_SPINDLE	195	5.61E-17	ABI1,RANBP9,SMC4,LRPPRC,WASF2,NET1,KATNB1,NDC80,TUBGCP3,ARFGEF1,CENPE,CENPF,SEPTIN9,RALBP1,KIF2C,CNTRL,KATNA1,CDC42EP1,TUBGCP5,FGD4,DYNLL2,PPP4R2,SASS6,DLG1,DYNC1H1,ECT2,EPB41,EPB41L2,MAPRE1,RAB3GAP1,TPX2,STK38L,KIF1B,FLNA,CLASP1,CD2AP,RABGAP1,KIF4A,FBXO5,RACGAP1,APC,BIRC5,INCENP,KIF3C,KIF5B,ARF6,KIF11,KIF22,ARHGAP5,LMNB1,MARCKS,MID1,MYH9,MYO1E,MYO9B,NCK1,NEK2,NF1,NOTCH2,OPHN1,PAFAH1B1,GEMIN4,PCNT,TUBD1,NIN,PLK1,ANLN,CEP192,CCDC88A,CEP72,CDK5RAP2,CENPJ,KIF15,ALS2,RASA2,RFC1,ROCK1,BCR,PLEKHG2,SOS1,SPTBN1,BRCA2,STAU1,AURKA,BUB1,TIAM1,TOP2A,TRIO,TTK,VCL,YWHAE,ALMS1,ARHGAP10,PIF1,ACTN4,SMC1A,NCK2,SSH2,ARHGEF7,WASF1,LATS1,SMC3,CCNB2,ARHGEF2,RASAL2,KIF23,KIF20B,ESPL1,CEP57,KNTC1,RAPGEF5,DLGAP5,CKAP5,CDK1,TLK1,CDC27,CDC42
HALLMARK_MYC_TARGETS_V2	56	7.62E-12	RCL1,CDK4,PRMT3,MPHOSPH10,MYBBP1A,NOP56,PLK4,CBX3,PPRC1,WDR43,RRP12,PES1,GNL3,UTP20,TMEM97,NDUFAF4,HK2,SLC29A2,HSPD1,HSPE1,MCM4,MCM5,MYC,NPM1,PA2G4,MRTO4,NIP7,NOP16,PHB1,PLK1,WDR74,TFB2M,SLC19A1,SRM,SUPV3L1,TCOF1,BYSL,UNG,AIMP2,DDX18,NOLC1,TBRG4,IMP4
HALLMARK_UNFOLDED_PROTEIN_RESPONSE	113	1.26E-11	PREB,PDIA6,HYOU1,NOP56,CEBPG,PAIP1,MTHFD2,PDIA5,KDELR3,XPOT,CKS1B,DCTN1,DDX10,DKC1,EIF2S1,EIF4E,EIF4G1,SEC31A,EXOSC2,SEC11A,EDC4,SERP1,PSAT1,ERO1A,H2AX,HSPA5,HSPA9,IARS1,KIF5B,ASNS,ATF4,NFYA,NFYB,CNOT4,NPM1,GEMIN4,EXOSC9,EXOSC10,SDAD1,DNAJC3,CNOT6,ALDH18A1,SRPRB,SSR1,TARS1,HSP90B1,VEGFA,YWHAZ,CHAC1,CALR,SLC7A5,KHSRP,NOP14,NOLC1,EIF2AK3,EIF4A3,TATDN2
HALLMARK_EPITHELIAL_MESENCHYMAL_TRANSITION	199	8.51E-09	CDH6,CDH11,FSTL3,MYL9,POSTN,COL1A1,COL1A2,COL3A1,COL5A1,COL5A2,COL6A2,COL6A3,COL7A1,COL8A2,COL16A1,COMP,LRRC15,DCN,ECM2,ELN,EMP3,FBLN1,FBN1,FUCA1,ABI3BP,GEM,GPC1,EFEMP2,IGFBP2,IGFBP4,CCN1,ITGB5,JUN,RHOB,LAMA2,LGALS1,LOXL1,LRP1,LUM,MATN3,MGP,MMP2,MSX1,GADD45B,NNMT,OXTR,COL5A3,PCOLCE,PDGFRB,PMP22,HTRA1,MAGEE1,ACTA2,CXCL12,SFRP4,SGCD,BMP1,SLIT3,SPARC,TGFB1,THY1,TIMP1,TPM2,VEGFC,ADAM12,MFAP5,PDLIM4,SLIT2
HALLMARK_SPERMATOGENESIS	94	3.42E-08	PARP2,CDKN3,DBF4,KIF2C,TOPBP1,DMC1,CSNK2A2,EZH2,HSPA4L,MAST2,LPIN1,NCAPH,MTOR,CNIH2,AGFG1,IDE,IL12RB2,ART3,MLF1,NEK2,NF2,STRBP,CHFR,PRKAR2A,RFC4,GMCL1,AURKA,BUB1,TSN,TTK,VDAC3,MLLT10,CLPB,COIL,PSMG1,CCNB2,CDK1
HALLMARK_PROTEIN_SECRETION	96	2.47E-07	TOM1L1,DNM1L,ADAM10,BET1,ARFGEF2,ARFGEF1,YKT6,CTSC,TMED2,RER1,VPS45,AP2M1,AP3S1,CLCN3,CLTA,CLTC,COPB1,AP2B1,AP1G1,ABCA1,SEC31A,DOP1A,MON2,KIF1B,STX12,SGMS1,ARFGAP3,ARF1P1,GNAS,GOLGA4,YIPF6,IGF2R,ARCN1,ARF1,LAMP2,LMAN1,M6PR,ATP1A1,OCRL,RAB14,ATP6V1H,PPT1,MAPK1,RAB22A,RAB2A,RAB5A,RPS6KA3,SH3GL2,BNIP3,SOD1,VAMP7,TPD52,STAM,TMX1,ANP32E,STX7,USO1,GBF1,NAPG,ZW10,COPB2,RAB9A,VPS4B,SEC22B,SCRN1,SEC24D

Supplement 1 data. ***Contidued*** **...**

ID	setSize	pvalue	geneID
HALLMARK_GLYCOLYSIS	188	9.17E-07	GNPDA1,GNE,KIF20A,SLC25A13,B3GNT3,BPNT1,HAX1,CENPA,KDELR3,ADORA2B,NANP,CTH,DLD,DSC2,ENO1,AK4,EXT1,EXT2,FKBP4,PAXIP1,ZNF292,SLC35A3,G6PD,SLC37A4,GALK2,GFPT1,GOT1,GOT2,GYS1,ERO1A,HDLBP,HK2,HMMR,HSPA5,IDH1,KIF2A,STMN1,LDHA,CHST6,MDH1,MDH2,ME1,ME2,NASP,P4HA1,NSDHL,PFKP,PGAM1,PGK1,PKM,PKP2,PLOD1,PLOD2,PMM2,PPIA,CLN6,PGM2,DEPDC1,PRPS1,PSMC4,PYGB,RRAGD,RARS1,RPE,SDHC,SOD1,SOX9,AURKA,TALDO1,TGFA,TPI1,TXN,UGP2,VEGFA,VLDLR,SRD5A3,B4GALT4,B4GALT2,SAP30,P4HA2,COPB2,HOMER1,HS2ST1,CDK1,MED24
HALLMARK_PI3K_AKT_MTOR_SIGNALING	101	2.49E-06	ACTR3,ACTR2,CDK2,CDK4,CFL1,AP2M1,CLTC,DDIT3,E2F1,EIF4E,PIKFYVE,AKT1,PLCB1,DAPP1,GNGT1,TBK1,GSK3B,ARF1,SMAD2,MYD88,ATF1,NCK1,PDK1,CAB39,PLCG1,PPP1CA,PPP2R1B,PRKAR2A,MAPK1,MAPK8,MAP2K3,RPTOR,TRIB3,PTPN11,RAC1,RAF1,RPS6KA3,SLC2A1,MAP3K7,TIAM1,HSP90B1,UBE2D3,UBE2N,YWHAB,MAPKAP1,CALR,PIK3R3,RIPK1,CDK1
HALLMARK_COAGULATION	117	1.21E-05	RAPGEF3,PRSS23,COMP,CRIP2,CTSH,CTSK,CTSO,TMPRSS6,CFD,F2RL2,F3,F8,F10,FBN1,MSRB2,ISCU,ANG,GSN,CFH,HPN,CFI,KLKB1,LRP1,MMP2,MMP11,MMP14,MST1,SERPINE1,PECAM1,SERPINA1,PLAT,PROC,PROS1,HTRA1,S100A13,,CFB,BMP1,SPARC,THBD,TIMP1,TIMP3,SERPING1,C1R,C3,VWF,CASP9
HALLMARK_DNA_REPAIR	148	1.19E-05	ALYREF,POLR3C,POLD3,SF3A3,TMED2,CLP1,NUDT21,ZWINT,CSTF3,DDB1,DGUOK,AGO4,ERCC3,FEN1,NCBP2,ARL6IP1,GTF2A2,GTF2H1,GTF2H3,SEC61A1,HPRT1,LIG1,NFX1,PNP,PCNA,NT5C3A,NELFCD,POLA1,POLD1,POLH,POLR2C,POLR2D,POLR2K,PRIM1,RAD51,RALA,REV3L,RFC2,RFC3,RFC4,RFC5,RPA2,SDCBP,UPF3B,SSRP1,STX3,TAF6,TAF13,ELOA,TYMS,UMPS,VPS37B,RAE1,RNMT,GTF3C5,POLR1C,POM121
HALLMARK_MYOGENESIS	187	2.17E-05	HDAC5,SORBS3,FST,SORBS1,COL1A1,COL3A1,COL6A2,COL6A3,COX7A1,CTF1,AEBP1,CFD,DMPK,APLNR,AK1,FHL1,FKBP1B,GAA,SH2B1,GPX3,GSN,HRC,IGF1,IGFBP7,ITGA7,ITGB5,LAMA2,LSP1,MEF2D,GADD45B,MYH3,MYL3,PPP1R3C,BAG1,SGCA,SGCD,SPARC,TGFB1,TPM2,VIPR1,OCEL1,ADAM12,CASQ1,CASQ2,BHLHE40,STC2,PDLIM7,CD36
HALLMARK_OXIDATIVE_PHOSPHORYLATION	198	2.10E-05	LRPPRC,TIMM17A,ACAA2,MTX2,PRDX3,AFG3L2,IMMT,PHB2,COX7A2,COX10,CPT1A,CS,CYC1,DLAT,DLD,DLST,ETFA,ALAS1,ABCB7,FH,NNT,FXN,HTRA2,GPI,MRPL15,SLC25A5,HADHA,HCCS,HSPA9,ACADM,IDH2,IDH3A,LDHA,LDHB,MDH1,MDH2,MTRR,NDUFA9,NDUFAB1,NDUFB3,NDUFB5,NDUFS1,NQO2,OAT,OGDH,OPA1,ATP5F1A,ACO2,ATP5F1B,ATP5F1C,MRPL35,ATP5PB,PDHA1,MPC1,ATP5MC3,SLC25A3,PHYH,ATP6V1C1,CYCS,POLR2F,POR,PDP1,MRPS22,TOMM22,SDHB,SDHC,SDHD,MRPS15,MRPS11,MRPL11,SUPV3L1,UQCRB,UQCRC2,UQCRFS1,UQCRH,VDAC1,VDAC2,VDAC3,GRPEL1,PDHX,ISCA1,SUCLG1,AIFM1,COX7A2L,TIMM50,COX5A,TOMM70,MFN2
HALLMARK_ESTROGEN_RESPONSE_EARLY	199	5.29E-05	DLC1,PRSS23,PLAAT3,CISH,ABAT,EGR3,ABCA3,KDM4B,FOS,SEC14L2,SLC39A6,LRIG1,MYOF,GFRA1,TJP3,RHOD,HES1,IGFBP4,IL6ST,AR,MAST4,KRT18,KRT19,MAPT,MUC1,NBL1,NPY1R,PDZK1,PGR,RETREG1,SYBU,MINDY1,OLFML3,BAG1,RARA,BCL2,ELOVL5,KCNK15,SCNN1A,CXCL12,RAB17,BLVRB,SIAH2,SLC7A2,SLC22A5,SULT2B1,TFF1,TFF3,TPBG,UGCG,WFS1,XBP1,CA12,SEMA3B,MLPH,ASB13,THSD4,ANXA9,BHLHE40,STC2,CCN5,FCMR,PTGES,CELSR1,GREB1
HALLMARK_UV_RESPONSE_UP	153	7.93E-05	PARP2,PPIF,CDK2,SIGMAR1,CEBPG,YKT6,STARD3,BTG3,STIP1,CHKA,PDAP1,CHRNA5,KLHDC3,CLCN2,NKX2-5,CTSV,E2F5,EIF2S3,EIF5,MARK2,ALAS1,FEN1,FKBP4,AMD1,GCH1,AGO2,GLS,H2AX,HNRNPU,DNAJA1,DNAJB1,ICAM1,LYN,EPCAM,ASNS,GAL,ATP6V1C1,POLE3,PPAT,PPP1R2,PSMC3,BAK1,RAB27A,RFC4,RPN1,BID,SLC6A8,HSPA13,TAP1,TARS1,TFRC,TYRO3,GRPEL1,CYB5B,CASP3,GGH,CCNE1,PRPF3,DDX21,LHX2,TGFBRAP1,NUP58,CDC5L